

Polymer Chemistry

Accepted Manuscript



This is an *Accepted Manuscript*, which has been through the Royal Society of Chemistry peer review process and has been accepted for publication.

Accepted Manuscripts are published online shortly after acceptance, before technical editing, formatting and proof reading. Using this free service, authors can make their results available to the community, in citable form, before we publish the edited article. We will replace this *Accepted Manuscript* with the edited and formatted *Advance Article* as soon as it is available.

You can find more information about *Accepted Manuscripts* in the [Information for Authors](#).

Please note that technical editing may introduce minor changes to the text and/or graphics, which may alter content. The journal's standard [Terms & Conditions](#) and the [Ethical guidelines](#) still apply. In no event shall the Royal Society of Chemistry be held responsible for any errors or omissions in this *Accepted Manuscript* or any consequences arising from the use of any information it contains.



Polymer Chemistry

ARTICLE

Synthesis, Characterization, and Field-Effect Transistors Properties of Tetrathienoanthracene-Based Copolymers Using A Two-Dimensional π -Conjugation Extension Strategy: A Potential Building Block for High-Mobility Polymer Semiconductors

Received 00th January 20xx,
Accepted 00th January 20xx

DOI: 10.1039/x0xx00000x

www.rsc.org/

Chao Li,^{a,#} Naihang Zheng,^{b,#} Huajie Chen,^{*a} Jianyao Huang,^b Zupan Mao,^b Liping Zheng,^a Chao Weng,^a Songting Tan^a and Gui Yu^{*b}

In most instances, modulation of the π -conjugation length in polymer molecules is obtained through a linear (1D) extension of the polymer backbone. To date, very limited studies have been reported about the effect of the two-dimensional (2D) π -conjugation extension on the charge-transporting properties of polymer semiconductors. In this study, a 2D π -extended heteroacene, alkyl-substituted tetrathienoanthracene (TTB) moiety, is used to design and synthesize a class of novel polymer semiconductors for solution-processable organic field-effect transistors (OFETs) applications first. Three novel TTB-based alternating copolymers (PTTB-2T, PTTB-TT, and PTTB-BZ) are synthesized via Pd(0)-catalyzed Stille or Suzuki cross-coupling reactions, affording high weight-average molecular weights of 61.1~78.5 kDa. The thermal stabilities, optical properties, and energy levels, and charge transport properties of the three TTB-based alternating copolymers have been successfully tuned by copolymerizing with bithiophene (2T), thienothiophene (TT), and benzothiadiazole (BZ) derivatives. The results indicate that, even with their highly extended π -framework, all the TTB-containing polymers show good solubility in most common solvents and fairly good environmental stability of their highest occupied molecular orbitals (HOMOs) ranging from -5.15 to -5.28 eV. Among the three TTB-based alternating copolymers, PTTB-BZ thin film exhibits the best OFETs performance with the highest hole mobility of $0.15 \text{ cm}^2 \text{ V}^{-1} \text{ s}^{-1}$ in ambient air. It can be attributed to the combinations of highly coplanar polymer backbones and strong D-A interactions between TTB donor units and BZ acceptor units, therefore leading to a compact solid-state packing, uniformly fiber-like morphology, large polycrystalline grain associated with high hole mobility. These results demonstrate that our molecular design strategy for high-performance polymer semiconductors is highly promising.

Introduction

Owing to the excellent solution processability, film uniformity, and thermal stability as well as the unique optoelectronic properties, π -conjugated polymer semiconductors have been intensively investigated as the key elements for realizing low-cost, flexible, and large-area organic electronics, such as organic light-emitting diodes (OLEDs), organic field-effect transistors (OFETs), and organic solar cells (OSCs).¹⁻¹¹ Among them, OFETs are the fundamental components for the next generation of organic electronics, which

can be applied into flexible large-area displays, integrated circuits, and radio frequency identification tags.¹⁻¹¹ Recently, great achievements have been made in solution-processable polymer-based OFETs with excellent charge carrier mobilities over $8.0 \text{ cm}^2 \text{ V}^{-1} \text{ s}^{-1}$ and relatively good device stabilities in ambient air,^{4,5} exhibiting a bright prospect in the field of organic electronics applications. However, the development of novel π -conjugated polymer semiconductors with unique structures still plays an important role in revealing the basic rules between polymer structure and performance as well as further improving charge transport performance, which could make great contributions to the commercial applications of OFETs in the future.

Recent research indicates that, to enhance the charge carrier mobility, π -conjugated polymers with highly fused aromatics have been attracted considerable attention as the most viable materials for OFETs applications.²⁻¹¹ Generally, the use of these rigid aromatic rings in polymer semiconductors can not only reduce the conformational disorder but also can facilitate the interchain π - π stacking of polymer backbones,¹²⁻¹⁴ which can be helpful for charge

^a Key Laboratory of Advanced Functional Polymeric Materials of College of Hunan Province, and Key Laboratory of Environmentally Friendly Chemistry and Applications of Ministry of Education, College of Chemistry, Xiangtan University, Xiangtan 411105, P. R. China. E-mail: chenhjoe@163.com.

^b Beijing National Laboratory for Molecular Sciences, Chinese Academy of Sciences, Beijing 100190, P. R. China. E-mail: yugui@iccas.ac.cn.

† Mr. C. Li and Mr. N. Zheng contributed equally to this work.

Electronic Supplementary Information (ESI) available: Synthetic details of TTB-2Br monomer, AFM phase images, and DFT calculation data. See DOI: 10.1039/x0xx00000x

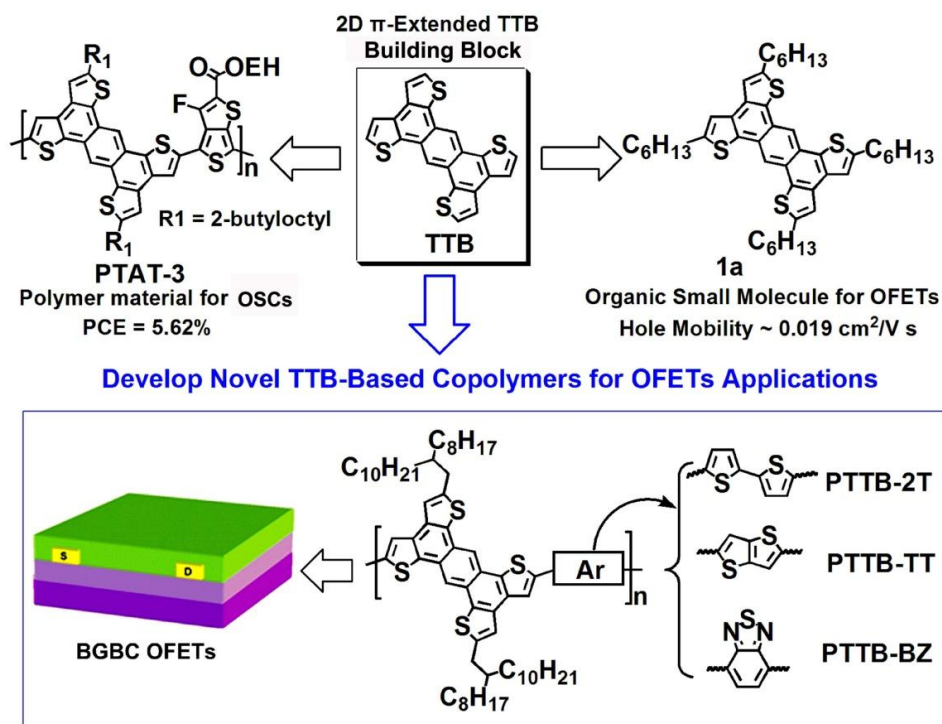


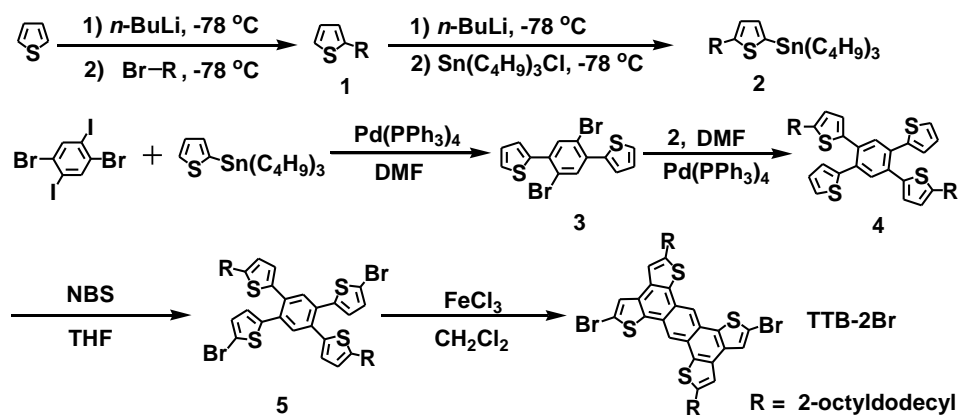
Fig. 1 Molecular structures of 2D π -extended TTB building block and its derivatives (PTAT-3 and 1a), and three novel TTB-based polymers (PTTB-2T, PTTB-TT, and PTTB-BZ) for solution-processed BGBC OFETs applications.

hopping through the face-to-face π -stacked polymer backbones. On the other hand, the construction of alternating donor-acceptor (D-A) backbones provides another effective method to achieve close intermolecular π - π stacking and effective charge hopping.⁵⁻¹¹ Consequently, an increasing number of D-A alternating copolymers containing highly fused aromatics had been reported for high-performance OFETs applications, such as thiophenylvinylthiophene-based (TVT),¹⁵⁻²⁰ indacenodithiophene-based (IDT),²¹⁻²³ isoindigo-based (IDG),²⁴⁻²⁹ diketopyrrolopyrrole-based (DPP),³⁰⁻³⁹ naphthalenediimide-based (NDI),⁴⁰⁻⁴⁵ and perylenediimide-based (PDI) polymer semiconductors.⁴⁶⁻⁴⁹ In most cases, modulation of the π -conjugation length in polymer semiconductors was attained through a linear (1D) elongation of the polymer backbones.¹⁻¹¹ To the best of our knowledge, there are very few investigations on the effect of the two-dimensional (2D) conjugation extension on the charge transport properties of polymer semiconductors.⁵⁰⁻⁵³ To explore novel strategies for further improving charge transport performance and probing the relationships between structure and property, the effect of dimensionality of π -conjugated system on OFETs performance is worthy of being studied systematically.

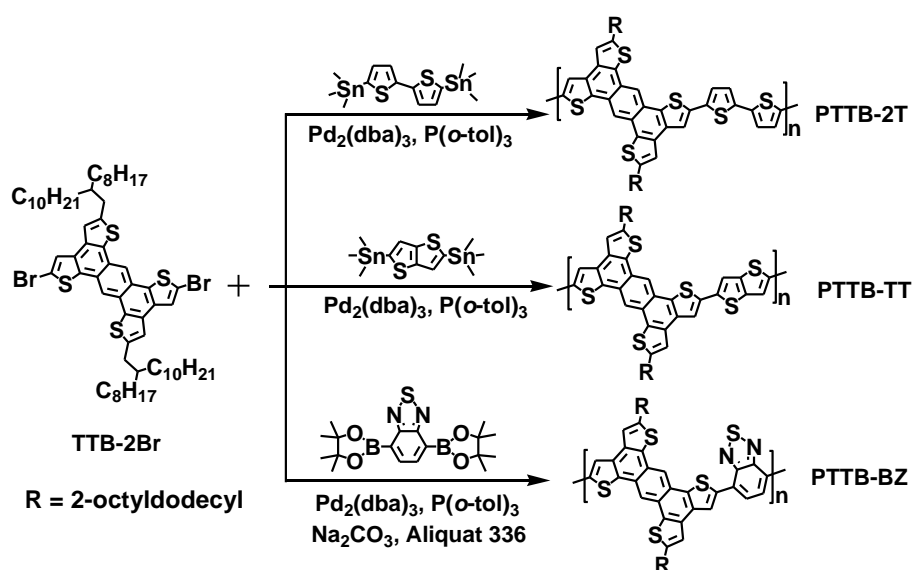
2D π -extended heteroacenes, alkyl-substituted tetrathienoanthracene derivatives (TTB, Figure 1), are well-known building blocks that have been successfully applied in developing organic small molecule semiconductors for OFETs^{54,55} and photoconductive polymer materials for OSCs applications,⁵¹ which showed hole mobility of $\sim 0.019 \text{ cm}^2 \text{ V}^{-1} \text{ s}^{-1}$ and photovoltaic efficiencies of 5.62%, respectively. Recently, on the basis of TTB modular structure, a series of 2D π -extended small molecule semiconductors have been reported on their device performances

of OFETs, exhibiting fairly good charge transport performance.⁵⁵⁻⁶¹ In view of their large electron delocalization system, good coplanarity, facile synthesis and purification as well as modular structure, 2D π -extended TTB moiety and its derivatives exhibit great potential in designing and synthesizing a wide range of highly π -extended polymer semiconductors for solution-processable OFETs applications. However, to our surprise, very limited studies have been reported so far for TTB-based polymers as semiconducting materials in OFETs.⁵¹ The incorporation of 2D π -extended TTB building block into the polymer backbone may enhance the cofacial π - π stacking of polymer backbones, which can facilitate high-performance charge transport.

Herein, we reported the design and synthesis of the three novel π -conjugated copolymers (PTTB-2T, PTTB-TT, and PTTB-BZ, see Fig. 1) based on 2D π -extended TTB building block, where simple bithiophene (2T), thienothiophene (TT), and benzothiadiazole (BZ) units were used as the linker unit to clearly understand the nature of TTB moieties when incorporated into the polymer backbone. Moreover, the comparative studies would be performed to reveal the effect of the different repeat units and different comonomers on their thermal stabilities, optical properties, energy levels, and thin film microstructures of the various TTB-based polymers by thermogravimetric analysis (TGA), ultraviolet-visible spectroscopy (UV-Vis), cyclic voltammetry (CV), atomic force microscope (AFM), and X-ray diffraction (XRD) measurements. The results revealed that, compared with PTTB-2T and PTTB-TT, the D-A type polymer PTTB-BZ exhibited higher thermal stability, more uniformly fiber-like morphology, larger polycrystalline grain as well as closer π - π



Scheme 1. Synthetic route for the monomer TTB-2Br.



Scheme 2 Synthetic route for the three TTB-based polymers.

stacking distance, and therefore featuring higher hole mobility of up to $0.15 \text{ cm}^2 \text{ V}^{-1} \text{ s}^{-1}$. The study demonstrated that, for the first time, the three novel polymer semiconductors containing 2D TTB-containing can be applied into the high-performance OFETs successfully.

Experimental

Materials

All chemicals were purchased from Chem Greatwall and Alfa Aesar, and used without further purification. Tetrahydrofuran (THF) and toluene were distilled from sodium. The compounds 5,5'-bis(trimethylstannyl)-2,2'-bithiophene,⁶² 2,5-bis(trimethylstannyl)-thieno[3,2-*b*]thiophene,¹² 2,1,3-benzothiadiazole-4,7-bis(boronic acid pinacol ester),⁶³ 3-tri-*n*-butylstannyl-5-(2-octyldodecyl)thiophene (2),⁶⁴ and 1,4-bis(2-thienyl)-2,5-dibromobenzene (3)⁵¹ were synthesized according to the reported procedures, respectively. The improved synthetic procedures for

the monomer 2,9-dibromo-5,12-di(2'-octyldodecyl)-trithieno[2',3':5,6:3',2':3,4:3',2':7,8]anthrax[1,2,*b*] thiophene (TTB-2Br) were provided in Supporting Information, which are similar to the previously reported procedures.⁵¹

Synthesis of PTTB-2T

To a 25 mL Schlenk tube, $\text{Pd}_2(\text{dba})_3$ (9 mg), $\text{P}(o\text{-tol})_3$ (14 mg), TTB-2Br (224 mg, 0.2 mmol), bis(trimethylstannyl)-2,2'-bithiophene (98.4 mg, 0.2 mmol), and 5 mL of toluene were added. This Schlenk tube was then charged with N_2 using a freeze-pump-thaw cycle technique to remove O_2 for three times. The mixture was stirred at 115°C for 48 h under a N_2 atmosphere. After cooling to room temperature, the polymer was precipitated from a mixture solution of methanol (300 mL) and hydrochloric acid (15 mL), and collected by filtration and washed with methanol. The crude polymer was further purified by Soxhlet extraction with methanol, acetone, hexane, and finally chloroform. A golden solid was obtained after removing chloroform (203 mg, 90%). GPC: $M_n = 39.3 \text{ kDa}$, $M_w = 77.8$

ARTICLE

Polymer Chemistry

kDa, PDI = 1.98. Elemental analysis calcd. for $(C_{70}H_{94}S_6)_n$: C 74.54; H 8.40; found: C 75.85, H 8.54%.

Synthesis of PTTB-TT

To a 25 mL Schlenk tube, $Pd_2(dba)_3$ (9 mg), $P(o\text{-tol})_3$ (14 mg), TTB-2Br (224 mg, 0.2 mmol), 2,5-bis(trimethylstannyl)thieno[3,2-*b*]thiophene (93.2 mg, 0.2 mmol), and 5 mL of toluene were added. This mixture solution was then charged with N_2 for three times by using a freeze-pump-thaw cycle technique, then stirred at 115 °C for 48 h under a N_2 atmosphere. After cooling to room temperature, the reaction mixture was added into 200 mL of menthol containing 10 mL of hydrochloric acid. The crude polymer solid was collected via filtration and further purified by Soxhlet extraction with methanol, acetone, hexane, and finally chloroform. Then the chloroform solution was evaporated and dried to yield a golden solid (205 mg, 93%). GPC: $M_n = 32.8$ kDa, $M_w = 78.5$ kDa, PDI = 2.39. Elemental analysis calcd. for $(C_{68}H_{92}S_6)_n$: C 74.12, H 8.42; found: C 75.48, H 8.65%.

Synthesis of PTTB-BZ

To a 25 mL Schlenk tube, $Pd_2(dba)_3$ (9 mg), $P(o\text{-tol})_3$ (14 mg), TTB-2Br (224 mg, 0.2 mmol), 2,1,3-benzothiadiazole-4,7-bis(boronic acid pinacol ester) (77.6 mg, 0.2 mmol), a drop of methyl trioctyl ammonium chloride (Aliquat 336), and 5 mL of toluene were added. This mixture was degassed with argon for 30 min, followed by the addition of Na_2CO_3 solution (2 mL, 2.5 M). The resultant mixture was degassed for another 10 min and then refluxed for 48 h. After cooling to room temperature, the reaction mixture was poured into 200 mL of methanol containing 15 mL of hydrochloric acid and stirred for 3 h. The crude polymer was collected via filtration and washed with 50 mL of methanol and 50 mL of hexane. The crude polymer was further purified by Soxhlet extraction with methanol, acetone, hexane, and finally chloroform. A deep blue solid was obtained after removing chloroform (160 mg, 73 %). GPC: $M_n = 32.5$ kDa, $M_w = 61.1$ kDa, PDI = 1.88. Elemental analysis calcd. For $(C_{68}H_{92}N_2S_5)_n$: C 74.40, H 8.45, N, 2.55; found: C 73.68, H 8.66, N 2.58%.

Instruments

Nuclear magnetic resonance (NMR) spectra were recorded on a Bruker Avance 400 instrument (400 MHz), using tetramethylsilane ($\delta = 0$ ppm) as the internal standard. MALDI-TOF mass spectrometric measurements were collected on a Bruker Autoflex III instrument. Elemental analysis was performed on a Valid EL-III element analyzer. Number-average and weight-average molecular weights were determined on a Waters 1515 gel permeation chromatograph (GPC) system using chloroform as an eluent and narrow polydispersity polystyrene as a standard. The concentrate of GPC samples was 1 mg mL⁻¹. UV-Vis measurements were conducted on a Perkin-Elmer Lamada 25 spectrometer. TGA measurements were performed on a Netzsch TG 209 analyzer with a heating rate of 10 °C min⁻¹ under an inert atmosphere. CV measurements were carried out in a conventional three-electrode cell using a platinum wire counter electrode and an Ag/AgCl (saturated KCl) reference electrode on an electrochemistry workstation (CHI660A, Chenhua Shanghai) at room temperature. The working electrode is a platinum stick coated with a layer of

polymer thin film. The scan rate was 100 mV s⁻¹, and a N_2 -saturated acetonitrile solution of 0.1 M tetrabutylammonium hexylfluorophosphate was used as the supporting electrolyte. All the potentials were calibrated with the standard ferrocene/ferrocenium redox couple. The potential of this external standard was determined to be 0.4 V under the same conditions. AFM measurements were carried out on a Nanoscope V instrument in a tapping mode. XRD experiments of thin film samples were performed on a BRUKER AXS D8 Advance diffractometer with a 40 kV FL tubes as the X-ray source (Cu K α) and the latest LYNXEYE XE detector.

OFETs fabrication and characterization

Solution-processed OFET devices were prepared by using bottom-gate bottom-contact (BGBC) test structures. A heavily doped silicon wafer with a layer of SiO_2 (300 nm) were used as a gate electrode and gate dielectric layer, respectively. The source-drain (D-S) electrodes (gold/titanium, 30 nm/5 nm) were prepared by photolithography, with the channel widths (W) of 1400 μm and channel lengths (L) of 10 μm . The silica substrates were hydrophobically modified by exposure in an oxygen plasma for 5 min and then cleaned in acetone, deionized water, and ethanol. Then the surface of SiO_2 gate dielectrics was modified with octadecyltrichlorosilane (OTS) in a vacuum. After that, the OTS-modified substrates were placed on a hot plate at 60 °C; and the polymer thin films (~30 nm) were prepared by drop-casting polymer solutions in *o*-dichlorobenzene (*o*-DCB, 10 mg mL⁻¹) at 60 °C. For annealing treatments, film samples were further placed on the hot plate at 220 °C for 5 minutes in ambient air directly. The charge carrier mobility of the thin films was assessed by measuring transfer curves in saturation, using a Keithley Model 4200 SCS semiconductor parameter analyzer in ambient air. The relative humidity of ambient air is 20~40 %. The field-effect mobility in saturation (μ) is calculated from equation:

$$I_{DS} = (W/2L) C_i \mu (V_{GS} - V_{th})^2$$

where W/L is the channel width/length, C_i is the gate dielectric layer capacitance per unit area, and V_{GS} and V_{th} are the gate voltage and threshold voltage, respectively.

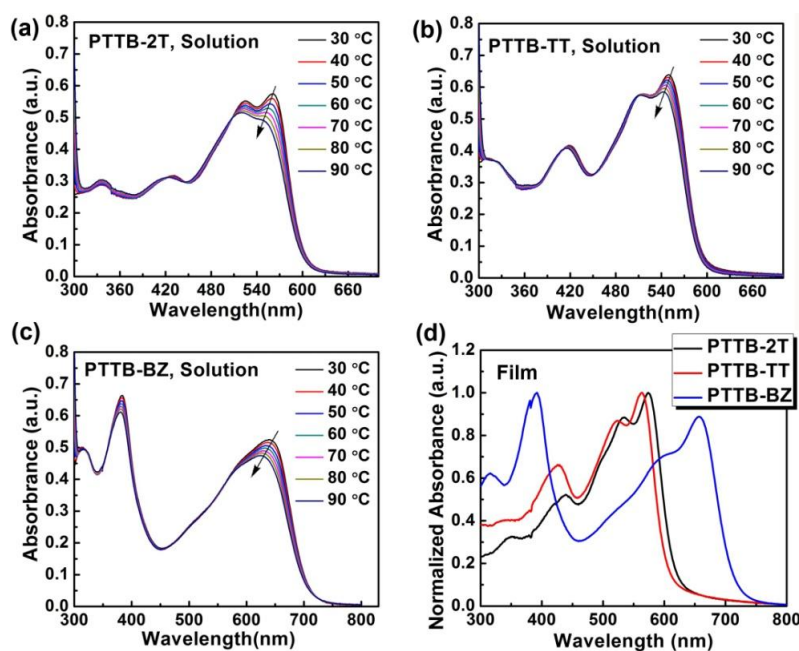
Results and Discussions**Synthesis and characterization**

Schemes 1 and 2 illustrate the synthetic routes for monomer TTB-2Br and three TTB-based copolymers, respectively. Firstly, 1,4-dibromo-2,5-diiodobenzene was reacted with 2-tri-*n*-butylstannylthiophene by Stille cross-coupling reaction to obtain compound 3 in 70% yield. Then another Stille cross-coupling reaction was applied to attach two 5-(2'-decyltetradecyl)-2-thienyl groups onto the compound 3, obtaining compound 4. After the dibromination of compound 4 with *N*-bromosuccinimide (NBS) in THF, the key intermediate 5 was obtained in a high yield. The intermediate 5 was then carried out the intramolecular cyclization: by anhydrous $FeCl_3$ oxidation to give the goal monomer TTB-2Br in 45% yield. Since the purification of monomers can obviously affect molecular weight and quality of the resulting polymers, all the comonomers were carefully recrystallized three times. All the

Table 1 Molecular weights, thermal stabilities, optical properties, and electrochemical properties of the different TTB-based polymers.

| Polymer | M_n/M_w (kDa) ^a | T_d (°C) | Solution λ_{max} (nm) | Film λ_{max} (nm) | $E_g^{optical}$ (eV) ^b | E_{ox}^{onset} (V) | E_{HOMO} (eV) | E_{LUMO} (eV) |
|---------|---------------------------------|------------|----------------------------------|------------------------------|--------------------------------------|-------------------------|--------------------|--------------------|
| PTTB-2T | 39.3/77.8 | 415 | 338, 431, 525, 562 | 439, 535, 574 | 1.95 | 0.75 | -5.15 | -3.20 |
| PTTB-TT | 32.8/78.5 | 425 | 418, 513, 550 | 428, 523, 564 | 2.0 | 0.78 | -5.18 | -3.18 |
| PTTB-BZ | 32.5/61.1 | 428 | 383, 643 | 392, 600, 656 | 1.68 | 0.88 | -5.28 | -3.60 |

^aDetermined by GPC and reported as their polystyrene equivalents. ^bDetermined by the onset of thin films absorption and estimated from the following equation: $E_g^{optical} = 1240/\lambda_{abs, onset}$.

**Fig. 2** (a–c) UV-Vis absorption spectra of the various TTB-based polymers in the diluted *o*-DCB solution and (d) as-cast thin film on quartz.

TTB-based copolymers were synthesized via Pd(0)-catalyzed Suzuki or Stille cross-coupling reactions, then purified by precipitation from acidic methanol and followed by Soxhlet extraction using methanol, acetone, hexane, and finally chloroform. The weight-average molecular weights (M_w) of the polymers, evaluated by GPC in chloroform at room temperature, were 77.8 kDa for PTTB-2T, 78.5 kDa for PTTB-TT, and 61.1 kDa for PTTB-BZ. Polydispersity indexes (PDIs) were determined to be 1.88–2.39. According to M_w , the degrees of polymerization (DP) of the polymers were calculated to be 55–71. It is well-known for other polymers that the charge carrier mobility might drop significantly due to their low molecular weights.¹⁰ For the three TTB-based polymers, however, the M_w values should be sufficient to explore these polymers-based OFETs performance. Additionally, the structure of the three TTB-based polymers was characterized by elemental analysis and ¹H NMR (see Figures S1–S3†). At room temperature, PTTB-BZ exhibits excellent solubility (>15 mg mL⁻¹) in most common solvents, including THF, toluene, and other chlorinated solvents. However, PTTB-TT and PTTB-2T are only soluble in hot chlorinated solvents (>10 mg mL⁻¹ in chloroform, chlorobenzene, and *o*-DCB at 80 °C). In particular, they

tend to form polymer gel at room temperature, probably resulting from their highly π -extended polymer backbones which can readily lead to strong intermolecular interactions and backbone aggregations.¹⁵ As shown in Fig. S4†, thermal gravimetric analysis revealed the exceptional thermal stability for the three TTB-based polymers, with the decomposition temperature (5% weight loss) above 415 °C. Due to the incorporations of rigid thieno[3,2-*b*]thiophene fused-rings and 2,1,3-benzothiadiazole heterocyclic rings into the polymer backbones, PTTB-TT and PTTB-BZ exhibited higher decomposition temperatures than that of PTTB-2T.

Optical Properties

The solution and thin-film absorption spectra of the three TTB-based polymers are shown in Fig. 2. The relevant data are summarized in Table 1. In dilute *o*-DCB solution, all the polymers exhibited two distinct features, corresponding to an intramolecular charge transfer (ICT) transition at low energy band and a π - π^* transition at high energy band, respectively.⁶⁵ Compared to PTTB-TT

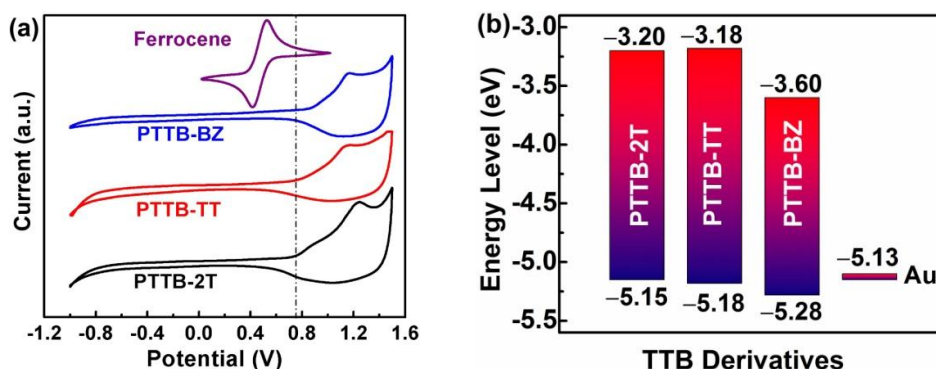


Fig. 3 (a) CV of the various TTB-based polymer thin films; (b) Experimental HOMO and LUMO energy levels for the compared systems.

solution (550 nm), PTTB-2T exhibited a red-shifted absorption peak at 562 nm. Moreover, obvious absorption shoulders at low energy band can be observed in both PTTB-TT and PTTB-2T polymer solutions, suggesting the strong aggregations of the polymer chains might be formed even in dilute *o*-DCB solutions.¹⁵ To elucidate this aggregation phenomenon, the situ temperature-controlled absorption spectra were measured at different temperatures as depicted in Fig. 2. Upon heating, clear change of the absorption spectra was observed for both PTTB-2T and PTTB-TT solutions, displaying a blue-shifted ICT peak and a reduced absorption intensity at low energy band. However, their absorption shoulders at low energy band still dominated even at 90 °C, indicating strong backbone aggregations can hardly remove in the polymer solutions even at 90 °C. The results corroborate the assumption of strong aggregation of the polymer chains in dilute *o*-DCB solutions. Because of strong ICT and D–A interactions, PTTB-BZ exhibited red-shifted ICT peak at 643 nm when compared to PTTB-2T and PTTB-TT. In their solid-state films, the absorption shoulders can be observed notably for all the TTB-based polymers. Moreover, the ICT peaks were all red-shifted (8~14 nm) and broadened than those of the solution spectra (see Table 1). This can be explained by a larger overlap of π orbitals due to better backbone aggregations in the solid-state films.¹⁵ Generally, this strong backbone aggregation will provide an effective channel for high-performance charge transport.¹⁵ As shown in Fig. 2d, the onset absorptions of the various TTB-based polymer thin films are determined to be ca. 635 nm for PTTB-2T, 620 nm for PTTB-TT, and 738 nm for PTTB-BZ. According to the following equation: optical bandgaps (E_g^{optical}) = $1240/\lambda_{\text{abs, onset}}^{[60]}$, the corresponding E_g^{optical} can be estimated to be 1.95 eV for PTTB-2T, 2.0 eV for PTTB-TT, and 1.68 eV for PTTB-BZ. Among the three TTB-based polymers, the smallest E_g^{optical} is achieved for PTTB-BZ, due to its strong ICT and D–A interaction between the electron-donating TTB unit and electron-withdrawing BZ unit through the whole polymer backbone.^{65–67}

Electrochemical Properties

Cyclic voltammetry was performed to measure the electrochemical behaviors of PTTB-2T, PTTB-TT, and PTTB-BZ, thereby determining their HOMO and LUMO energy levels. Fig. 3 displays the electrochemical properties of the three polymer thin films, and the corresponding CV data are collected in Table 1. Three polymers exhibited strong oxidation processes but weak reduction ones, in

good agreement with the electron-rich nature of polymer backbones.^{12–14} The HOMO and LUMO energy levels of the polymers could be calculated from the onset potentials of redox peaks relative to the oxidation potential of ferrocene external standard, as shown in the following equation: $\text{HOMO} = -[E_{\text{ox}}^{\text{onset}} + E_{\text{ox}}^{\text{onset}}(\text{ferrocene})] - 4.8 \text{ eV}$.⁶⁰ Under the same conditions, the onset oxidation potential of the ferrocene was determined to be 0.4 V. According to the respective onset oxidation potentials in Fig. 3a, the HOMO energy levels are determined to be –5.15 eV for PTTB-2T, –5.18 eV for PTTB-TT, and –5.28 eV for PTTB-BZ. Notably, the three TTB-based polymers exhibit relatively deep-lying HOMO values below –5.15 eV, much lower than that (–4.76 eV) of regioregular pol(3-hexylthiophene).⁶⁸ The low-lying HOMO energy levels match well with the Fermi level (5.13 eV) of Au source/drain electrode (see Fig. 4b),⁶⁹ thus facilitating hole injection from Au electrode to polymer thin films effectively. According to the E_g^{optical} , HOMO energy levels, and the empirical equation of $\text{LUMO} = (E_g^{\text{optical}} + \text{HOMO}) \text{ eV}$, the LUMO energy levels were estimated, with the corresponding values of –3.20 eV for PTTB-2T, –3.18 eV for PTTB-TT, and –3.60 eV for PTTB-BZ, respectively. As clearly displayed in Fig. 3b, PTTB-BZ exhibits much lower HOMO and LUMO values compared with those of PTTB-2T and PTTB-TT. The main reasons can be ascribed to stronger ICT as well as D–A interactions between the TTB-based electron donor units and BZ-based electron acceptor units.^{65–67}

Computational Study

In order to understand structural and electronic characteristics of the various TTB-based polymers, molecular orbitals and energy levels of the polymer repeat units were calculated by Density Functional Theory (DFT), using the Gaussian 03 program at the B3LYP 6-31G* level.⁷⁰ To shorten the calculation time, three repeat units of the polymers were chosen to optimize molecular structures. As shown in Fig. S5†, the three TTB-based polymers exhibit the dihedral angles of 1~17°, which are much smaller than those of other high-mobility polymers, including NDI-based polymers P(NID2OD-T2) and PNVTs (~40°).⁴³ The results indicated that the three TTB-based polymers had a relatively good backbone coplanarity, therefore featuring a strong tendency to aggregate even in dilute *o*-DCB solutions. Additionally, the well-delocalized HOMO and LUMO orbitals of the three repeat units (see Fig. 4)

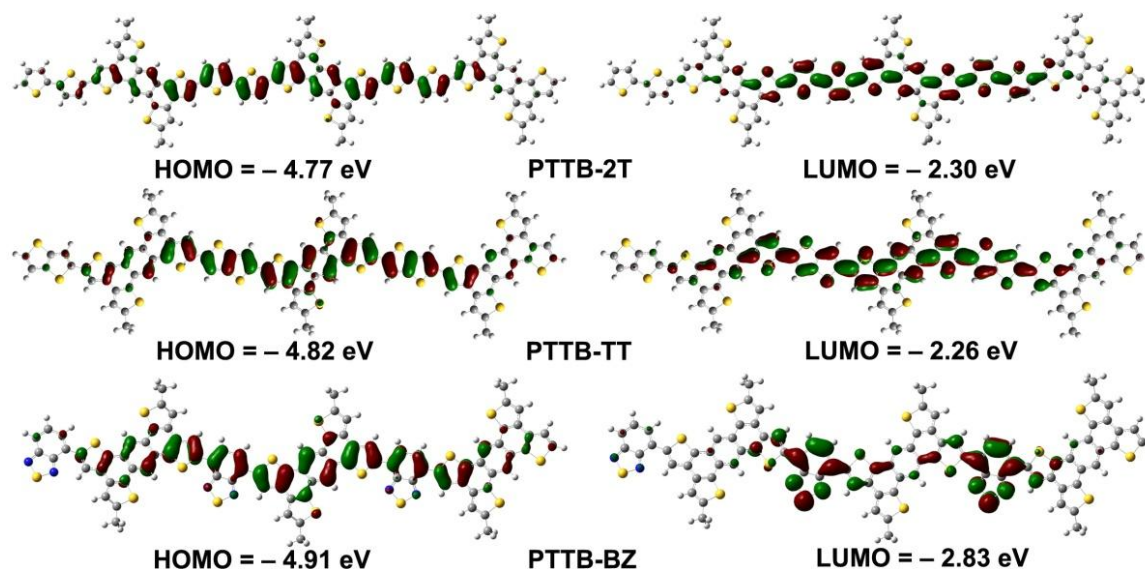


Fig. 4 Calculated molecular orbitals and HOMO/LUMO energy levels of the methyl-substituted PTTB-2T, PTTB-TT, and PTTB-BZ.

suggest that the polymer backbones of PTTB-2T and PTTB-TT possess high π -conjugations, which would facilitate charge carrier delocalization through the whole π -conjugation systems. For D–A type polymer PTTB-BZ, LUMO energy distribution seems to be mainly localized on the benzothiadiazole acceptor moieties, supporting the above-mentioned view of the stronger ICT interaction observed by UV–Vis spectroscopy. Additionally, the HOMO and LUMO energy levels of the polymer repeat units were also calculated, and the corresponding data are shown in Fig. 4. Note that the calculated HOMO and LUMO energy levels are different from the CV data of polymers (see Table 1), which might arise from the exciton bonding energy of the conjugated polymer.⁷¹ While the D–A type polymer PTTB-BZ still exhibits much lower HOMO and LUMO values than those of PTTB-TT and PTTB-2T, which is in accordance with the tendency of the CV data.

Thin Film Field-effect transistors

Polymer-based OFET devices with BGBC configurations were fabricated on the surface of OTS-modified Si/SiO₂ (300 nm) substrates. In ambient air, pronounced hole characteristics were found for the three TTB-based polymer thin films. Typical transistor transfer and output characteristics are shown in Fig. 5; and the obtained data are summarized in Table 2. The results indicate that the hole mobilities of the TTB-based polymers are dependent on the annealing temperature. Before annealing, the PTTB-TT based OFET devices exhibited relatively low average hole mobility of 0.004 cm² V⁻¹ s⁻¹, with the current on/off ratio (I_{on}/I_{off}) above 10³. Compared to PTTB-TT, the unannealed PTTB-BZ and PTTB-2T thin films afforded higher average hole mobilities of up to 0.008 and 0.02 cm² V⁻¹ s⁻¹, respectively. Such notable enhancement of hole mobility could be ascribed to larger crystal grains for both PTTB-2T and PTTB-BZ thin films than that of PTTB-TT, which was confirmed by AFM data below. After annealing at 220 °C for 5 min, three TTB-based polymer thin films exhibited the best hole transport performance. For PTTB-TT- and PTTB-2T-based OFET devices, the

calculated highest hole mobilities were equal to 0.03 and 0.08 cm² V⁻¹ s⁻¹, respectively. Compared with PTTB-TT and PTTB-2T, the D–A type polymer PTTB-BZ thin films exhibited better hole transport performance in ambient air. At a drain voltage (V_{DS}) of –80 V, the average hole mobility for the PTTB-BZ thin films annealed at 220 °C were 0.09 cm² V⁻¹ s⁻¹; and the maximum hole mobility reached 0.15 cm² V⁻¹ s⁻¹, two orders of magnitude higher than that before annealing. As clearly demonstrated in AFM and XRD data below, the combinations of increased polycrystalline grain size and crystallinity and decreased grain boundaries in their thin films after thermal annealing treatments have contributed to the increased hole transport ability.

Thin film morphology

To gain a better understanding of the effects of thermal annealing on the OFETs performance, the surface morphology of the polymer thin films, deposited on OTS-modified SiO₂/Si substrates, were performed by AFM in a tapping mode. Fig. 6 shows the surface topography images for as-cast and 220 °C-annealed films of the polymers; and phase images are shown in Fig. S6†. AFM topography and phase images revealed that the three TTB-based polymer thin films exhibited different morphology structures, consistent well with the difference of their charge transport abilities above. For both PTTB-2T and PTTB-TT thin films, nodule-like surface features were clearly observed, suggestive of some degree of backbone aggregation or crystallinity.¹⁵ However, PTTB-BZ thin films displayed typically fiber-like morphology, which is similar to most of high-performance polymer semiconductors, including DPP-based,^{30–39} IDG-based,^{24–29} and NDI-based polymers.^{40–45} Remarkably, PTTB-2T and PTTB-BZ thin films exhibited larger crystal grains when compared with PTTB-TT ones (see Fig. 6 and Fig. S6†), indicating that strong polymer backbone stacking and aggregation were formed in PTTB-2T and PTTB-BZ thin films. Generally, large crystal grain will facilitate charge transport.¹⁵ Therefore, PTTB-2T and

Table 2 BGBC OFET devices characteristics of the different TTB-based polymers

| Polymers | As-cast | | | Annealed at 220 °C | | | |
|----------|--|------------------------|--------------------------------|--|---|------------------------|--------------------------------|
| | μ_{aver}^a ($\text{cm}^2 \text{V}^{-1} \text{s}^{-1}$) | V_{th} (V) | $I_{\text{on}}/I_{\text{off}}$ | μ_{aver}^a ($\text{cm}^2 \text{V}^{-1} \text{s}^{-1}$) | μ_{max} ($\text{cm}^2 \text{V}^{-1} \text{s}^{-1}$) | V_{th} (V) | $I_{\text{on}}/I_{\text{off}}$ |
| PTTB-2T | 0.02 | -18 to -14 | $>10^3$ | 0.065 | 0.08 | -23 to -18 | $>10^3$ |
| PTTB-TT | 0.004 | -22 to -18 | $>10^3$ | 0.02 | 0.03 | -35 to -30 | $>10^3$ |
| PTTB-BZ | 0.008 | -15 to -12 | $>10^3$ | 0.09 | 0.15 | -34 to -28 | $>10^4$ |

^a Mobility statistics from more than 20 devices.

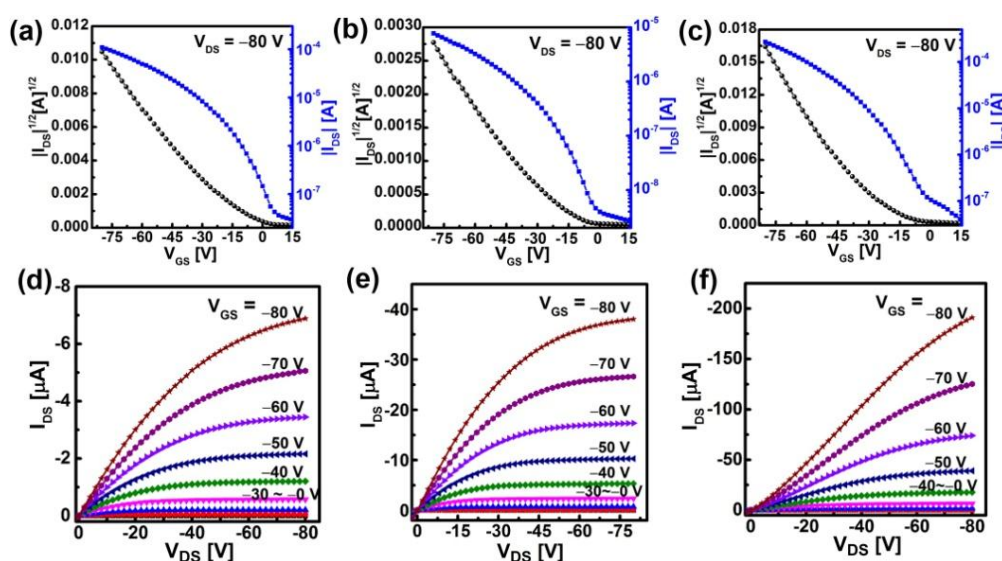


Fig. 5 Typical transfer (a~c) and output (d~f) curves of the OFET devices fabricated from the polymer thin films, (a, d) PTTB-2T, (b, e) PTTB-TT, and (c, f) PTTB-BZ.

PTTB-BZ thin films exhibited better charge transport performances than that of PTTB-TT. Additionally, upon annealing, root-mean-square roughness (RMS) values of the three TTB-based polymers were enhanced (see Fig. 6 and Fig. S7[†]), therefore featuring larger polycrystalline grain and higher hole mobility when compared with as-cast thin films. However, when the annealing temperature reached at 240 °C, PTTB-BZ thin films displayed larger polycrystalline grain size but worse film interconnectivity due to deep crystalline boundary (see Fig. S7[†]), and therefore resulting in a reduced hole mobility.

Film crystalline and microstructure To explain the differences of OFETs performance, film crystallinity and microstructure are also critical parameters.²⁻¹¹ Therefore, the three TTB-based polymers thin films, deposited on OTS-modified SiO₂/Si substrates, were further studied by XRD measurements. Fig. 7 shows the typical diffraction plots of as-cast films and annealed films. As shown in Fig. 7, the three polymer thin films, annealed at 220 °C, exhibit clear 100 and 010 diffraction peaks. Moreover, the 010 diffraction signals were obviously enhanced after annealing treatments. This result suggested that the degrees of crystallinity of the polymer thin films were enhanced after annealing treatment. The enhancement of the

thin film crystallinity would be helpful for charge transport.²⁻¹¹ After annealing at 220 °C, the three TTB-based polymers exhibited clear 100 diffraction peaks at $2\theta = 4.83^\circ$ for PTTB-TT, 4.77° for PTTB-2T, and 4.76° for PTTB-BZ. The corresponding lamellar distance are 18.27 Å for PTTB-TT, 18.50 Å for PTTB-2T, and 18.43 Å for PTTB-BZ. The observed lamellar distances are much shorter than that of fully extended alkyl side chains, suggesting that the side chains are closely interdigitated with the other side chains in adjacent layers.^{15,36} On the basis of the data obtained from PTTB-BZ thin films annealed at 220 °C, a (010) feature at $2\theta = 25.6^\circ$, corresponding to the π - π stacking distance of 3.48 Å, were demonstrated, which was smaller than those of PTTB-TT ($2\theta = 25.4^\circ$, 3.53 Å) and PTTB-2T ($2\theta = 25.2^\circ$, 3.50 Å) thin films. The shorter π - π stacking distance suggested the strongly intermolecular interactions in PTTB-BZ thin films, which can be accounted for the strong π - π stacking of highly π -extended polymer backbones as well as strong D-A interactions. In combination with the advantages of uniformly fiber-like morphologies and large polycrystalline grains for PTTB-BZ thin films, the compact lamellar stacking structure has contributed to charge hopping through the face-to-face π -stacked polymer backbones. Therefore, PTTB-BZ and PTTB-2T thin films exhibited higher hole mobilities than that of PTTB-TT one.

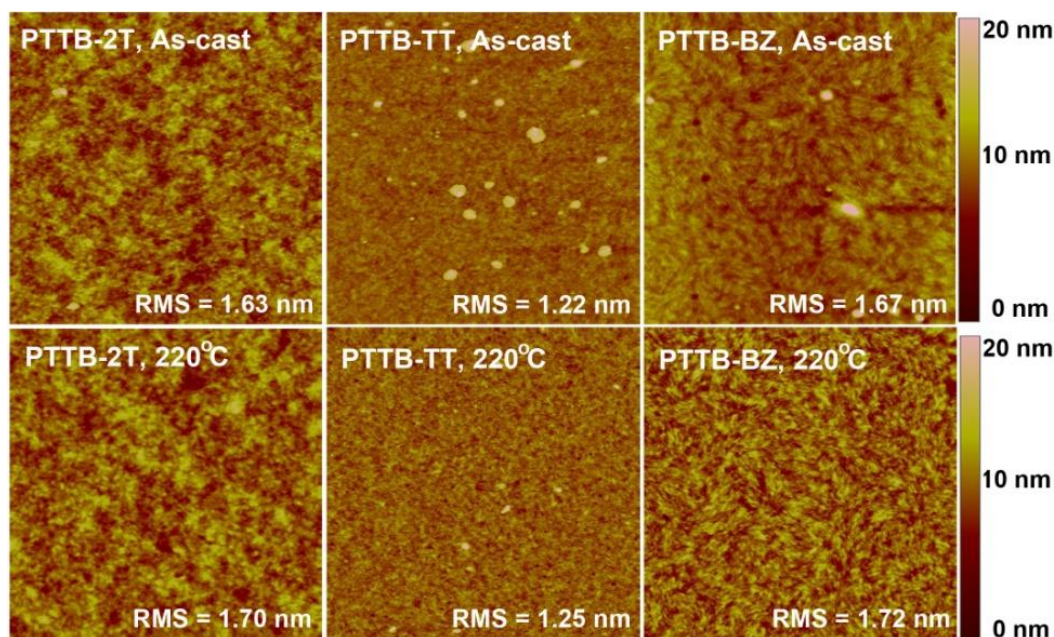


Fig. 6 AFM topography images ($5 \times 5 \mu\text{m}$) of as-cast (top row) and annealed (bottom row) TTB-based polymer thin films. The root-mean-squared roughness of each thin films is indicated in nm.

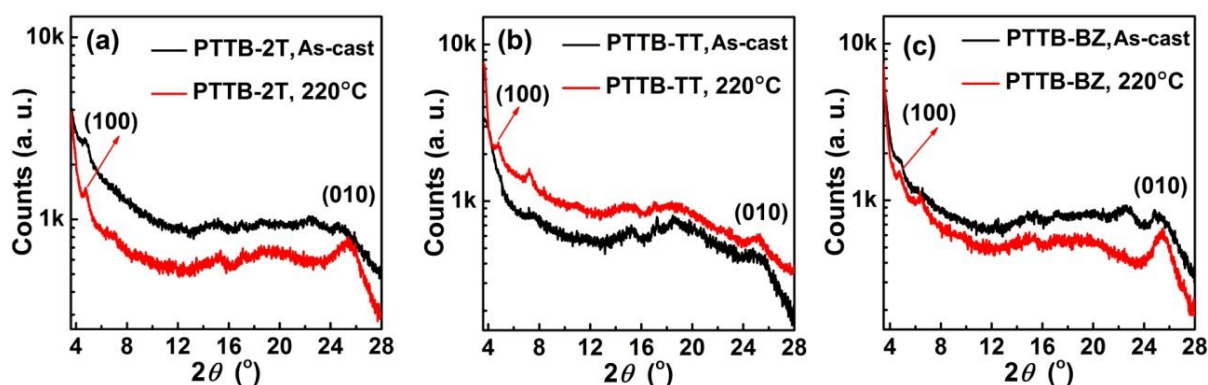


Fig. 7 XRD patterns of the polymer thin films deposited on the OTS-modified SiO_2/Si substrates.

Conclusions

In summary, we reported a simple and facile synthesis for the preparation of 2D π -extended TTB derivatives containing branched alkyl side chains at the thiophene α -positions. We also demonstrated that this kind of 2D π -extended derivative monomers (TTB-2Br) could be copolymerized with 2T, TT and BZ derivatives by the Pd(0)-catalyzed Stille or Suzuki cross-coupling reactions to afford polymers with high weight-average molecular weights of 61.1~78.5 kDa. The thermal stabilities, optical properties, HOMO/LUMO energy levels, and film microstructures of the three TTB-based polymers had been successfully characterized by TGA, UV-Vis, CV, AFM, and XRD measurements. The experimental results indicated that the resulting polymers exhibited an exceptional thermal stability ($T_d > 415 \text{ }^\circ\text{C}$), good solution processability, low-lying HOMO energy levels below -5.15 eV , well delocalized conjugation backbone associated with close π - π stacking structures.

According to their absorption spectra and thin-film surface morphologies, clear evidence of backbone aggregation was observed. The results indicated that this orderly backbone aggregation had facilitated high-performance charge transport. Owing to the combinations of close solid-state packing, uniformly fiber-like morphology as well as large polycrystalline grain, the D-A type polymer PTTB-BZ exhibited the best hole transport performance among the three TTB-based polymers. In ambient air, the highest hole mobility of $0.15 \text{ cm}^2 \text{ V}^{-1} \text{ s}^{-1}$ was demonstrated for PTTB-BZ thin films. To the best of our knowledge, the hole mobility of PTTB-BZ reported in this study is the highest mobility value among the reported polymer semiconductors with 2D π -extended building blocks. These features in the resulting polymers offer great interest of using 2D π -extended TTB derivative units as the building blocks for polymer semiconductors and provide new insight into designing a new class of 2D π -extended polymer semiconductors with unique optoelectronic properties. Further investigation on the

applications of PTTB-BZ in OFET and OSC devices and the usage of 2D π -extended building block for the construction of novel D-A polymer semiconductors are undergoing.

Acknowledgements

This work was supported by the Natural Science Foundation of Hunan Province (Grants No. 2015JJ3122), the National Natural Science Foundation of China (Grants No. 51403177, 51233006, and 21474081), the National Science Foundation for Post-doctoral Scientists of China (Grant No. 2014M552141), and the Research Foundation of Education College of Hunan Province, China (Grant No. 14C1091).

Notes and references

- J. Zaumseil, H. Sirringhaus, *Chem. Rev.*, 2007, **107**, 1296–1323.
- P. M. Beaujuge, J. M. J. Fréchet, *J. Am. Chem. Soc.*, 2011, **133**, 20009–20029.
- C. L. Wang, H. L. Dong, W. P. Hu, Y. Q. Liu, D. B. Zhu, *Chem. Rev.*, 2012, **112**, 2208–2267.
- J. G. Mei, Y. Diao, A. L. Appleton, L. Fang, Z. N. Bao, *J. Am. Chem. Soc.*, 2013, **135**, 6724–6746.
- X. G. Guo, A. Facchetti, T. J. Marks, *Chem. Rev.*, 2014, **114**, 8943–9021.
- T. Lei, J. Y. Wang, J. Pei, *Acc. Chem. Res.*, 2014, **47**, 1117–1126.
- S. Holliday, J. E. Donaghey, I. McCulloch, *Chem. Mater.*, 2014, **26**, 647–663.
- J. F. M. Hardigree, H. E. Katz, *Acc. Chem. Res.*, 2014, **47**, 1369–1377.
- K. Takimiya, I. Osaka, M. Nakano, *Chem. Mater.*, 2014, **26**, 587–593.
- H. N. Tsao, D. M. Cho, I. Park, M. R. Hansen, A. Mavrinskiy, D. Y. Yoon, R. Graf, W. Pisula, H. W. Spiess, K. Müllen, *J. Am. Chem. Soc.*, 2011, **133**, 2605–2612.
- Z. T. Liu, G. X. Zhang, Z. X. Cai, X. Chen, H. W. Luo, Y. H. Li, J. G. Wang, D. Q. Zhang, *Adv. Mater.*, 2014, **26**, 6965–6977.
- I. McCulloch, M. Heeney, C. Bailey, K. Genevicius, I. MacDonald, M. Shkunov, D. Sparrowe, S. Tierney, R. Wagner, W. M. Zhang, M. L. Chabinyc, R. L. J. Kline, M. D. McGehee, M. F. Toney, *Nat. Mater.*, 2006, **5**, 328–333.
- Z. P. Fei, P. Pattanasattayavong, Y. Han, B. C. Schroeder, F. Yan, R. J. Kline, T. D. Anthopoulos, M. Heeney, *J. Am. Chem. Soc.*, 2014, **136**, 15154–15157.
- H. J. Chen, C. He, G. Yu, Y. Zhao, J. Y. Huang, M. L. Zhu, H. T. Liu, Y. L. Guo, Y. F. Li, Y. Q. Liu, *J. Mater. Chem.*, 2012, **22**, 3696–3698.
- H. J. Chen, Y. L. Guo, G. Yu, Y. Zhao, J. Zhang, D. Gao, H. T. Liu, Y. Q. Liu, *Adv. Mater.*, 2012, **24**, 4618–4622.
- I. Kang, H. J. Yun, D. S. Chung, S. K. Kwon, Y. H. Kim, *J. Am. Chem. Soc.*, 2013, **135**, 14896–14899.
- H. J. Yun, S. J. Kang, Y. Xu, S. O. Kim, Y. H. Kim, Y. Y. Noh, S. K. Kwon, *Adv. Mater.*, 2014, **26**, 7300–7307.
- X. T. Liu, Y. L. Guo, Y. Q. Ma, H. J. Chen, Z. P. Mao, H. L. Wang, G. Yu, Y. Q. Liu, *Adv. Mater.*, 2014, **26**, 3631–3636.
- H. J. Yun, G. B. Lee, D. S. Chung, Y. H. Kim, S. K. Kwon, *Adv. Mater.*, 2014, **26**, 6612–6616.
- H. Li, X. D. Wang, F. B. Liu, H. B. Fu, *Poly. Chem.*, 2015, **6**, 3283–3289.
- W. M. Zhang, J. Smith, S. E. Watkins, R. Gysel, M. McGehee, A. Salleo, J. Kirkpatrick, S. Ashraf, T. Anthopoulos, M. Heeney, I. McCulloch, *J. Am. Chem. Soc.*, 2010, **132**, 11437–11439.
- X. R. Zhang, H. Bronstein, A. J. Kronemeijer, J. Smith, Y. Kim, R. J. Kline, R. J. Richter, T. D. Anthopoulos, H. Sirringhaus, K. Song, M. Heeney, W. M. Zhang, I. McCulloch, D. M. DeLongchamp, *Nat. Commun.*, 2013, **4**, 2238.
- C. Luo, A. K. K. Kyaw, L. A. Perez, S. Patel, M. Wang, B. Grimm, G. C. Bazan, E. J. Kramer, A. J. Heeger, *Nano Lett.*, 2014, **14**, 2764–2771.
- T. Lei, Y. Cao, Y. L. Fan, C. J. Liu, S. C. Yuan, J. Pei, *J. Am. Chem. Soc.*, 2011, **133**, 6099–6101.
- J. G. Mei, D. H. Kim, A. L. Ayzner, M. F. Toney, Z. N. Bao, *J. Am. Chem. Soc.*, 2011, **133**, 20130–20133.
- R. S. Ashraf, A. J. Kronemeijer, D. I. James, H. Sirringhaus, I. McCulloch, *Chem. Commun.*, 2012, **48**, 3939–3941.
- G. Kim, S. J. Kang, G. K. Dutta, Y. K. Han, T. J. Shin, Y. Y. Noh, C. Yang, *J. Am. Chem. Soc.*, 2014, **136**, 9477–9483.
- B. He, A. B. Pun, D. Zherebetsky, Y. Liu, F. Liu, L. M. Klivansky, A. M. McGough, B. A. Zhang, K. Lo, T. P. Russell, L. W. Wang, Y. Liu, *J. Am. Chem. Soc.*, 2014, **136**, 15093–15101.
- X. Zhou, N. Ai, Z. H. Guo, F. D. Zhuang, Y. S. Jiang, J. Y. Wang, J. Pei, *Chem. Mater.*, 2015, **27**, 1815–1820.
- J. C. Bijleveld, A. P. Zoombelt, S. G. J. Mathijssen, M. M. Wienk, M. Turbiez, D. M. de Leeuw, R. A. J. Janssen, *J. Am. Chem. Soc.*, 2009, **131**, 16616–16617.
- J. S. Ha, K. H. Kim, D. H. Choi, *J. Am. Chem. Soc.*, 2011, **133**, 10364–10367.
- H. Bronstein, Z. Y. Chen, R. S. Ashraf, W. M. Zhang, J. P. Du, J. R. Durrant, P. S. Tuladhar, K. Song, S. E. Watkins, Y. Geerts, M. M. Wienk, R. A. J. Janssen, T. Anthopoulos, H. Sirringhaus, M. Heeney, I. McCulloch, *J. Am. Chem. Soc.*, 2011, **133**, 3272–3275.
- J. D. Yuen, J. Fan, J. Seifter, B. Lim, R. Hufschmid, A. J. Heeger, F. Wudl, *J. Am. Chem. Soc.*, 2011, **133**, 20799–20807.
- J. Li, Y. Zhao, H. S. Tan, Y. Guo, C. -A. Di, G. Yu, Y. Q. Liu, M. Lin, S. H. Lim, Y. Zhou, H. Su, B. S. Ong, *Sci. Rep.*, 2012, **2**, 754.
- T. W. Lee, D. H. Lee, J. Shin, M. J. Cho, D. H. Choi, *Poly. Chem.*, 2015, **6**, 1777–1785.
- Y. N. Li, S. P. Singh, P. Sonar, *Adv. Mater.*, 2010, **22**, 4862–4866.
- H. J. Yun, J. Cho, D. S. Chung, Y. H. Kim, S. K. Kwon, *Macromolecules*, 2014, **47**, 7030–7035.
- B. Sun, W. Hong, Z. Q. Yan, H. Aziz, Y. N. Li, *Adv. Mater.*, 2014, **26**, 2636–2642.
- R. S. Ashraf, I. Meager, M. Nikolka, M. Kirkus, M. Planells, B. C. Schroeder, S. Holliday, M. Hurhangee, C. B. Nielsen, H. Sirringhaus, I. McCulloch, *J. Am. Chem. Soc.*, 2015, **137**, 1314–1321.
- H. Yan, Z. Chen, Y. Zheng, C. Newman, J. R. Quinn, F. Dötz, M. Kastler, A. Facchetti, *Nature*, 2009, **457**, 679.
- M. S. Szumilo, E. H. Gann, C. R. McNeill, V. Lemaire, Y. Oliver, L. Thomsen, Y. Vaynzof, M. Sommer, H. Sirringhaus, *Chem. Mater.*, 2014, **26**, 6796–6804.
- A. Luzio, D. Fazzi, F. Nübling, R. Matsidik, A. Straub, H. Komber, E. Giussani, S. E. Watkins, M. Barbatti, W. Thiel, E. Gann, L. Thomsen, C. R. McNeill, M. Caironi, M. Sommer, *Chem. Mater.*, 2014, **26**, 6233–6240.
- H. J. Chen, Y. L. Guo, Z. P. Mao, G. Yu, J. Y. Huang, Y. Zhao, Y. Q. Liu, *Chem. Mater.*, 2013, **25**, 3589–3596.
- R. Kim, B. Kang, D. H. Sin, H. H. Choi, S. K. Kwon, Y. H. Kim, K. Cho, *Chem. Commun.*, 2015, **51**, 1524–1527.
- X. G. Guo, F. S. Kim, M. J. Seger, S. A. Jenekhe, M. D. Watson, *Chem. Mater.*, 2012, **24**, 1434–1442.
- X. W. Zhan, A. Facchetti, S. Barlow, T. J. Marks, M. A. Ratner, M. R. Wasielewski, S. R. Marder, *Adv. Mater.*, 2011, **23**, 268–284.
- X. G. Zhao, L. C. Ma, L. Zhang, Y. G. Wen, J. M. Chen, Z. G. Shuai, Y. Q. Liu, X. W. Zhan, *Macromolecules*, 2013, **46**, 2152–2158.
- S. Vasimalla, S. P. Senanayak, M. Sharma, K. S. Narayan, P. K. Iyer, *Chem. Mater.*, 2014, **26**, 4030–4037.
- Y. J. Hwang, T. Earmme, B. A. E. Courtright, F. N. Eberle, S. A. Jenekhe, *J. Am. Chem. Soc.*, 2015, **137**, 4424–4434.
- H. Usta, C. Newman, Z. K. Chen, A. Facchetti, *Adv. Mater.*, 2012, **24**, 3678–3684.
- F. He, W. Wang, W. Chen, T. Xu, S. B. Darling, J. Strzalka, Y. Liu, L. P. Yu, *J. Am. Chem. Soc.*, 2011, **133**, 3284–3287.
- Z. -A. Li, Y. Zang, C. C. Chueh, N. Cho, J. R. Lu, X. Y. Wang, J. Huang, C. Z. Li, J. S. Yu, A. K. -Y. Jen, *Macromolecules*, 2014, **47**, 7407–7415.
- D. F. Dang, P. Zhou, J. Zhong, J. Fan, Z. R. Wang, Y. F. Wang, Y. Pei, X. C. Bao, R. Q. Yang, W. P. Hu, W. G. Zhu, *Polymer*, 2014, **55**, 6708–6716.
- W. J. Liu, Y. Zhou, Y. G. Ma, Y. Cao, J. Wang, J. Pei, *Org. Lett.*, 2007, **9**, 4187–4190.
- J. L. Brusso, O. D. Hirst, A. Dadvand, S. Ganesan, F. Ciccoira, C. M. Robertson, R. T. Oakley, F. Rosei, D. F. Perepichka, *Chem. Mater.*, 2008, **20**, 2484–2494.

- 56 Q. Ye, J. J. Chang, K. W. Huang, C. Y. Chi, *Org. Lett.*, 2011, **13**, 5960–5963.
- 57 Y. Zhou, W. J. Liu, Y. G. Ma, H. L. Wang, L. M. Qi, Y. Cao, J. Wang, J. Pei, *J. Am. Chem. Soc.*, 2007, **129**, 12386–12387.
- 58 J. Y. Wang, Y. Zhou, J. Yan, L. Ding, Y. G. Ma, Y. Cao, J. Wang, J. Pei, *Chem. Mater.*, 2009, **21**, 2595–2597.
- 59 S. M. Zhang, Y. L. Guo, Y. J. Zhang, R. G. Liu, Q. K. Li, X. W. Zhan, Y. Q. Liu, W. P. Hu, *Chem. Commun.*, 2010, **46**, 2841–2843.
- 60 J. Yin, Y. Zhou, T. Lei, J. Pei, *Angew. Chem. Int. Ed.*, 2011, **50**, 6320–6323.
- 61 Y. Cao, X. Y. Wang, J. Y. Wang, J. Pei, *Synlett*, 2014, **25**, 313–323.
- 62 D. E. Seitz, S. H. Lee, R. N. Hanson, J. C. Bottaro, *Synth. Commun.*, 1983, **13**, 121–128.
- 63 M. Zhang, H. N. Tsao, W. Pisula, C. Yang, A. K. Mishra, K. Müllen, *J. Am. Chem. Soc.*, 2007, **129**, 3472–3473.
- 64 Ellinger, S.; Ziener, U.; Thewalt, U.; Landfester, K.; Möller, M. *Chem. Mater.*, 2007, **19**, 1070–1075.
- 65 C. Li, Z. P. Mao, H. J. Chen, L. P. Zheng, J. Y. Huang, B. Zhao, S. T. Tan, G. Yu, *Macromolecules*, 2015, **48**, 2444–2453.
- 66 Q. H. Wu, M. Wang, X. L. Qiao, Y. Xiong, Y. G. Huang, X. K. Gao, H. X. Li, *Macromolecules*, 2013, **46**, 3887–3894.
- 67 Z. X. Cai, H. W. Luo, P. L. Qi, J. G. Wang, G. X. Zhang, Z. T. Liu, D. Q. Zhang, *Macromolecules*, 2014, **47**, 2899–2906.
- 68 J. H. Hou, Z. –A. Tan, Y. Yan, Y. J. He, C. H. Yang, Y. F. Li, *J. Am. Chem. Soc.*, 2006, **128**, 4911–4916.
- 69 B. R. Conrad, C. K. Chan, M. A. Loth, S. R. Parkin, X. Zhang, D. M. DeLongchamp, J. E. Anthony, D. J. Gundlach, *Appl. Phys. Lett.*, 2010, **97**, 133306.
- 70 *Gaussian 03, Revision C. 02*, M. J. Frisch, G. W. Trucks, H. B. Schlegel, G. E. Scuseria, M. A. Robb, J. R. Cheeseman, J. A. Montgomery, Jr., T. Vreven, K. N. Kudin, J. C. Burant, J. M. Millam, S. S. Iyengar, J. Tomasi, V. Barone, B. Mennucci, M. Cossi, G. Scalmani, N. Rega, G. A. Petersson, H. Nakatsuji, M. Hada, M. Ehara, K. Toyota, R. Fukuda, J. Hasegawa, M. Ishida, T. Nakajima, Y. Honda, O. Kitao, H. Nakai, M. Klene, X. Li, J. E. Knox, H. P. Hratchian, J. B. Cross, C. Adamo, J. Jaramillo, R. Gomperts, R. E. Stratmann, O. Yazyev, A. J. Austin, R. Cammi, C. Pomelli, J. W. Ochterski, P. Y. Ayala, K. Morokuma, G. A. Voth, P. Salvador, J. J. Dannenberg, V. G. Zakrzewski, S. Dapprich, A. D. Daniels, M. C. Strain, O. Farkas, D. K. Malick, A. D. Rabuck, K. Raghavachari, J. B. Foresman, J. V. Ortiz, Q. Cui, A. G. Baboul, S. Clifford, J. Cioslowski, B. B. Stefanov, G. Liu, A. Liashenko, P. Piskorz, I. Komaromi, R. L. Martin, D. J. Fox, T. Keith, M. A. Al-Laham, C. Y. Peng, A. Nanayakkara, M. Challacombe, P. M. W. Gill, B. Johnson, W. Chen, M. W. Wong, C. Gonzalez, and J. A. Pople, Gaussian, Inc., Wallingford CT, 2004.
- 71 N. S. Sariciftci, *Primary Photoexcitations in Conjugated Polymers: Molecular Excitons vs Semiconductor Band Model*; World Scientific: Singapore, 1997.